RADIAL GRAVITY ANOMALIES ASSOCIATED WITH SECONDARY CRATER CHAINS SURROUNDING THE ORIENTALE BASIN FOUND IN GRAIL DATA. J. C. Jansen[1], J. C. Andrews-Hanna[2,1], C. Milbury[3], Y. Li[1], H. J. Melosh[3], J. W. Head III[4], J. M. Soderblom[5], and M. T. Zuber[5], [1]Dept. of Geophysics, Colorado School of Mines, Golden, CO 80401, jjansen@mines.edu, [2]Soutwest Research Institute, Boulder, CO 80302, [3]Dept. of Earth, Atmospheric, and Planetary Sciences, Purdue University, West Lafayette, IN 47907, [4]Dept. of Earth, Environmental and Planetary Sciences, Brown University, Providence, RI 02912, [5]Dept. of Earth, Atmospheric, and Planetary Sciences, Massachusetts Institute of Technology, Cambridge, MA 02139.

Introduction: Since the acquisition of gravity data from the Gravity Recovery And Interior Laboratory (GRAIL) mission, many subsurface structures have been discovered, including linear features in the gravity gradients [1] and buried craters [2]. Here we discuss the gravitational signature of the linear structures radiating out from the Orientale Basin (Fig. 1). It has been noted that around Orientale lines of craters form radial chains similar to those seen around other smaller lunar craters [3], in places forming linear troughs [4], that are interpreted as secondary crater chains. GRAIL data now reveal both positive and negative gravity anomalies associated with these secondary crater chains, as well as radial gravity anomalies with no clear surface expression. Both the crater chains [4] and the radial gravity anomalies are observed around other basins as well, but are best preserved around Orientale.

Here we analyse the radial gravity anomalies seen in the GRAIL gravity data, and investigate possible sources. First we characterize the magnitude and sign of the radial gravity anomalies. Next we perform gravity inversions [5,6] to examine the associated density anomalies in the subsurface. Finally we look at the effects that low velocity impactors have on the density and porosity of the crust and determine whether this can explain the different signs of the density anomalies associated with the radial gravity anomalies.

Methods: The Bouguer gravity was first processed using a high-pass filter that is complimentary to the minimum amplitude filter used in crustal thickness modeling [7] in order to emphasize small-scale crustal density anomalies. We next identified radial structures at the surface in the Lunar Orbiter Laser Altimeter (LOLA) topography data and the Wide Angle Camera (WAC) global image mosaic, and, separately, radial gravity anomalies in the subsurface using GRAIL Bouguer gravity [8] and gravity gradients [1]. The gravity signatures were then classified as positive or negative in sign (indicating whether the underlying materials are more or less dense than the surrounding materials).

Next, for the gravity inversions, we used a 3D density inversion algorithm [5,6], to generate a three-dimensional density model from the observed gravity data. This model minimizes an objective function that relates the data misfit and the model smoothness with a regularization parameter [9]. Finally, we examined the possible role of the impact of Orientale ejecta in making the observed radial gravity anomalies [10]. The range of distances of the secondary crater chains from the center of Orientale was measured and used to calculate the range in vertical velocities upon impact for a range of assumed ejection angles [10]. Using the pi-scaling relationship and the range of secondary crater diameters found around Orientale, the typical range of projectile diameters impacting to form secondary crater chains was calculated. These ranges in impact parameters were then used as input in iSALE models of impacts for a range of initial porosities to examine the predicted changes in density for comparison with the gravity inversions

Results and interpretations: A Bouguer map of the Orientale Basin and its surroundings (Fig. 1) shows patterns of both positive and negative linear gravity anomalies radiating out from the center of the basin outside the Cordillera ring. A closer look at an area northwest of Orientale shows a chain of secondary craters (Fig. 2), Catena Leuschner (Fig. 2, top center outline) is associated with a positive signal in the filtered Bouguer. Catena Leuschner has a positive

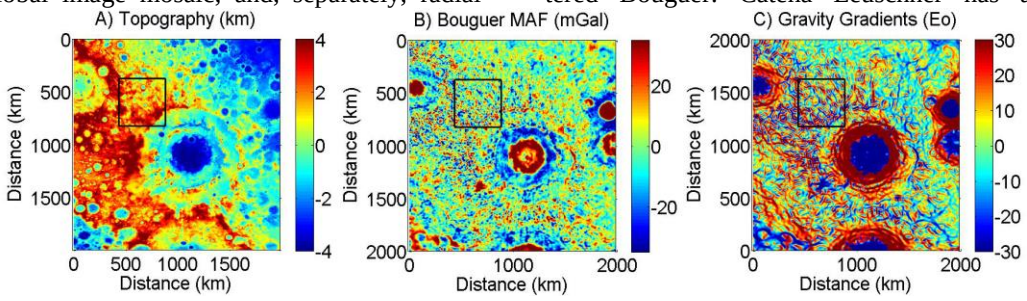

Figure 1. **A)** LOLA topography of the Orientale Basin (km), **B)** Complimentary minimum amplitude filtered Bouguer (mGal). **C)** Maximum gravity gradient (Eo). Study area O1 is outlined by the black box.

Bouguer anomaly of ~10 mGal which continues beyond the end of the visible crater chain to the southeast toward the interior of the Orientale Basin. Similarly, a number of radial features are observed in gravity where no feature is observed at the surface.

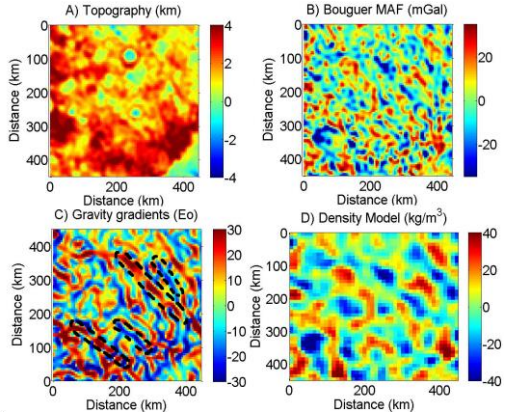

Figure 2. A) Topography (km), **B)** complimentary minimum amplitude filtered Bouguer (mGal), **C)** gravity gradient (Eo), including outlines of radial features, and **D)** Horizontal cross-section at 10 km depth of the density model (kg/m^3) of an area northwest of Orientale (see Fig. 1 for location).

Both positive and negative radial gravity anomalies are observed in the data. Closer to the basin (250-500 km from the basin center), radial gravity anomalies are more abundant and ~60% of them exhibit negative anomalies, while further out (750-1000 km from the basin center) ~75% of the radial gravity anomalies have positive signs.

The density model obtained by inverting the gravity predicts that the radial gravity anomalies are associated with density contrasts in the range of $\pm$40 kg/m^3 (Fig. 2). This density contrast is equivalent to a $\pm$1.5% change in porosity, though we cannot exclude other interpretations of the gravity anomalies such as variations in composition. The typical radial gravity anomalies are only a few 10's of km wide and extend to about 10-15 km depth.

For assumed ejection angles of the material forming the crater chains between 35° and 55°, and the observed range in distances of 250 to 1000 km from the center of the basin, we calculate vertical ejecta impact velocities of 380-1000 m/s. These velocities are much lower than typical hyper-velocity impacts forming primary craters [10]. Most of the secondary crater chains are found to have diameters ranging from 5 to 25 km, yielding impactor sizes between 0.5 and 7 km from the pi-scaling relationship.

Building on previous work [11], a number of impact models were run using these ranges in projectile velocity and diameter and assuming target porosities of 7, 12, and 17%. It was found that the predicted density anomalies imparted to the target are much smaller than the density anomalies resulting directly from the impacting material because much of the projectile material remains within the crater in these low velocity impacts. For a typical upper crust porosity of 12% [7], the effect of the remnant target material on the column-integrated density anomaly is approximately 10× greater than the effect of the compaction of the pore space in the target material. For the range of impact velocities expected in the formation of these crater chains, the effects of the velocity on the target density is small. Thus, we conclude that the most probable source for the linear radial gravity and density anomalies around Orientale is the presence of primary ejecta material excavated from the Orientale Basin within the rays themselves, rather than changes in the density of the target due to impacts.

Conclusions: GRAIL data shows linear gravity anomalies radiating out from the Orientale Basin, some of which are associated with secondary crater chains. Inversion of the these gravity anomalies reveals both positive and negative density anomalies of about $\pm$40 kg/m^3. Negative anomalies are more common closer to the basin and positive ones further out. Impact simulations show that the density of the impactors themselves dominate the density contrast of the secondary craters.

Orientale is surrounded by a low density annulus [7,12] corresponding to its ejecta deposit [13,14], indicating that the density of the impacting material responsible for the crater chains is also low. Closer to the center of the basin, where the material impacted at lower velocities [10], the majority of the radial gravity anomalies are negative. This observation is consistent with hydrocode model results which indicate that, at lower velocities, more secondary projectile material remains in the crater, and this material is of a low density. Further from the center of the basin, where ejecta impacts at higher velocity and less projectile material remains in the crater, the compaction as a result of the impacts may play a larger role and explain the predominance of positive gravity anomalies at those distances.

References: [1] Andrews-Hanna J. C. et al. (2013) *Science, 339, 6120*, 675-678. [2] Evans A. J. et al. (2015) *LPS XLVI*, Abstract #9052. [3] Wilhelms D. E. et al. (1978) *LPS IX*, 3735-3762. [4] Wilhelms D. E. (1976) *LPS XII*, 1883-2901. [5] Li Y. and Oldenburg D. (1996) *Geophys., 6*, 394-408. [6] Li Y. and Oldenburg D. (1998) *Geophys., 63*, 109-119. [7] Wieczorek M. A. (2013) *Science, 339*, 671-674. [8] Zuber M. T. et al (2013) *Science, 339*, 668-671 [9] Jansen J. C. (2014) *LPS* XLV Abstract #2730. [10] Oberbeck V. R. (1975) *U.S. Geol. Surv. Prof. Pap., 1348*, pp 302 [11] Milbury C. et al. (2015) *GRL*, doi:10.10022015GL066198. [12] Besserer J. (2014) *GRL, 41*, 5771-5777. [13] Scott D. H. et al. (1977) *U.S. Geol Surv. Misc. Inv. Series, I-1034*. [14] Wilhelms D. E. (1987) *U.S. Geol. Surv. Prof. Pap., 1348*, pp 302.